Chapter 7

Effect of Evapotranspiration on Hydrothermal Changes in Regional Scale

Tadanobu Nakayama

Additional information is available at the end of the chapter

http://dx.doi.org/10.5772/52808

1. Introduction

Evapotranspiration plays an important role not only on hydrologic cycle but also on thermal changes in various ways. In China, hydro-climate is diverse between north and south (Fig. 1). Semi-arid north is heavily irrigated and combination of increased food demand and declining water availability is creating substantial pressures in Yellow River (Brown and Halweil, 1998; Yang et al., 2004; Nakayama et al., 2006, 2010; Nakayama, 2011a, 2011b), whereas flood storage ability around lakes has decreased and impact of Three Gorges Dam (TGD) on flood occurrence in Changjiang downstream against original purpose is increasing problem in humid south (Shankman and Liang, 2003; Zhao et al., 2005; Nakayama and Watanabe, 2008b). Irrigation has a different impact on evapotranspiration changes at rotation between winter wheat and summer maize in the semi-arid region in the north (downstream of Yellow River), and double-cropping of rice in the humid south (middle of Changjiang River) in China. This mechanism changes greatly hydrologic cycle such as river discharge and groundwater, and in particular, affects extremes of flood and drought under climatic change (Nakayama, 2011a, 2011b, 2012c; Nakayama and Watanabe, 2006, 2008b; Nakayama et al., 2006, 2010).

On the other hand, urban heat island (Oke, 1987), where the urban temperature is higher than its rural surroundings, has become a serious environmental problem with the expansion of cities and industrial areas in the world (Fig. 1). Surfaces covered by concrete or asphalt can absorb a large amount of heat during the day and release it to the atmosphere at night. The evaporation of water provides an important counter to this effect, and so open parks and water surfaces are vital in urban areas for creating urban cool-island (Spronken-Smith and Oke, 1999; Chang et al., 2007). Recent researches showed that cooling effect of water-holding pavements made of new symbiotic material (consisting of porous asphalt and water-holding filler made of steel by-products based on silica compound) in addition to that of natural green

area on hydrothermal cycle is effective to recover sound hydrologic cycle and to create thermally-pleasing environments in eco-conscious society (Nakayama and Fujita, 2010; Nakayama and Hashimoto, 2011; Nakayama et al., 2007, 2012).

In this way, the evapotranspiration plays an important role on hydrologic change in continental basins where water resources are vital for human activity, and effective management of water resource is powerful for decision-making and adaptation strategy for sustainable development. This chapter represents the improvement in process-based National Integrated Catchment-based Eco-hydrology (NICE) model series (Nakayama, 2008a, 2008b, 2009, 2010, 2011a, 2011b, 2012a, 2012b, 2012c; Nakayama and Fujita, 2010; Nakayama and Hashimoto, 2011; Nakayama and Watanabe, 2004, 2006, 2008a, 2008b, 2008c; Nakayama et al., 2006, 2007, 2010, 2012) with more complex sub-systems to develop coupled human and natural systems and to analyze impact of evapotranspiration on hydrothermal changes in regional scale.

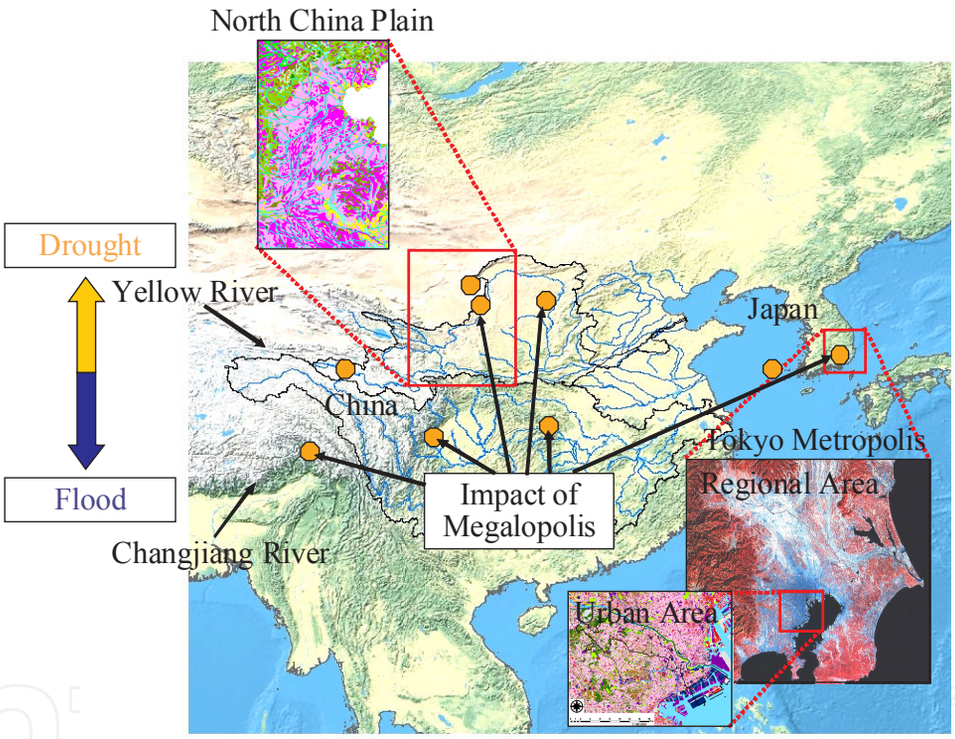

Figure 1. Study area in East Asia including the Changjiang and Yellow River basins in China, and the Tokyo Metropolis in Japan.

2. Material and methods

2.1. Coupling of process-based model with complex sub-systems

Previously, the author developed the process-based NICE model, which includes surface-unsaturated-saturated water processes and assimilates land-surface processes describing the

http://dx.doi.org/10.5772/52808

variations of LAI (leaf area index) and FPAR (fraction of photosynthetically active radiation) from satellite data (Fig. 2) (Nakayama, 2008a, 2008b, 2009, 2010, 2011a, 2011b, 2012a, 2012b, 2012c; Nakayama and Fujita, 2010; Nakayama and Hashimoto, 2011; Nakayama and Watanabe, 2004, 2006, 2008a, 2008b, 2008c; Nakayama et al., 2006, 2007, 2010, 2012). The unsaturated layer divides canopy into two layers, and soil into three layers in the vertical dimension in the SiB2 (Simple Biosphere model 2) (Sellers et al., 1996). About the saturated layer, the NICE solves three-dimensional groundwater flow for both unconfined and confined aquifers. The hillslope hydrology can be expressed by the two-layer surface runoff model including freezing/thawing processes. The NICE connects each sub-model by considering water/heat fluxes: gradient of hydraulic potentials between the deepest unsaturated layer and the groundwater, effective precipitation, and seepage between river and groundwater.

In agricultural field, NICE is coupled with DSSAT (Decision Support Systems for Agrotechnology Transfer) (Ritchie et al., 1998), in which automatic irrigation mode supplies crop water requirement, assuming that average available water in the top layer falls below soil moisture at field capacity for cultivated fields (Nakayama et al., 2006). The model includes different functions of representative crops (wheat, maize, soybean, and rice) and simulates automatically dynamic growth processes. Potential evaporation is calculated on Priestley and Taylor equation (Priestley and Taylor, 1972), and plant growth is based on biomass formulation, which is limited by various reduction factors like light, temperature, water, and nutrient, et al. (Nakayama et al., 2006; Nakayama and Watanabe, 2008b; Nakayama, 2011a).

In urban area, NICE is coupled with UCM (Urban Canopy Model) to include the effect of hydrothermal cycle at various pavements, and with RAMS (Regional Atmospheric Modeling System) (Pielke et al., 1992) to include the hydrothermal interaction (Nakayama and Fujita, 2010; Nakayama and Hashimoto, 2011; Nakayama et al., 2012). In particular, the author expanded specific heat conductivity c_s and heat conductivity k_s in natural soil (Sellers et al., 1996) for engineered pavement in the following equations by including the effect of water amount on the heat characteristics in the material.

$$\begin{aligned} c_s &= \left[0.5\left(1-\theta_s\right)+\theta_s \cdot W_1\right] C_w \cdot \rho_w \quad \textit{for soil} \\ &= C_p \cdot \rho_p \left(1-\theta_s\right) + C_w \cdot \rho_w \cdot \theta_s \cdot W_1 \quad \textit{for engineered pavement} \end{aligned} \tag{1}$$

$$\begin{aligned} k_s &= 0.4186 \frac{1.5\left(1-\theta_s\right)+1.3\theta_s \cdot W_1}{0.75+0.65\theta_s-0.4\theta_s \cdot W_1} \quad \textit{for soil} \\ &= k_p \left(1-\theta_s\right) + k_w \cdot \theta_s \cdot W_1 \quad \textit{for engineered pavement} \end{aligned} \tag{2}$$

C_p (J/kg/K) is specific heat of pavement material; C_w (J/kg/K) is specific heat of water (=4.18×10^6); c_s (J/m^3/K) is specific heat conductivity including the effect of water; k_s (W/m/K) is heat conductivity including the effect of water; k_p (W/m/K) is heat conductivity of pavement

material; k_w (W/m/K) is heat conductivity of water (=0.59); ρ_p (kg/m^3) is specific gravity of pavement material; ρ_w (kg/m^3) is density of water (=1,000), W_i is the soil moisture fraction of the i-th layer (=θ_i/θ_s); θ_s (m^3/m^3) is volumetric soil moisture in the i-th layer; θ_s (m^3/m^3) is the value of θ at saturation, respectively.

Downward short- and long-wave radiation, precipitation, atmospheric pressure, air temperature, air humidity, and wind speed simulated by the atmospheric model are input into the UCM, whereas momentum, sensible, latent, and long-wave flux simulated by the UCM are input into the atmospheric model at each time step. This procedure means that the feedback process about water and heat transfers between atmospheric region and land surface are implicitly included in the simulation process.

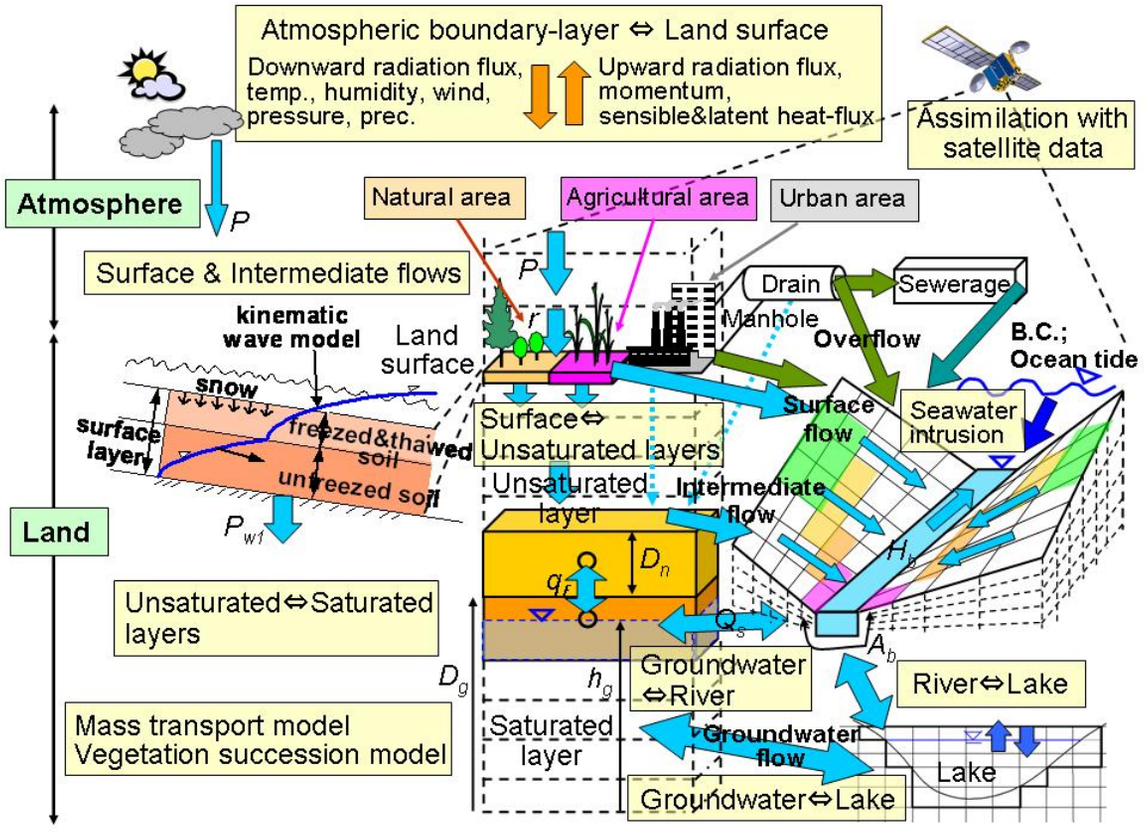

Figure 2. National Integrated Catchment-based Eco-hydrology (NICE) model.

2.2. Model input data and running the simulation

Six-hour re-analyzed data were input into the model after interpolation of ECMWF (European Centre for Medium-Range Weather Forecasts) in inverse proportion to the distance back-calculated in each grid. Because the ECMWF precipitation had the least reliability and underestimated observed peak values, rain gauge daily precipitation collected at meteorological stations were used to correct the ECMWF value (Nakayama, 2011a, 2011b, 2012c; Nakaya-

http://dx.doi.org/10.5772/52808

ma and Watanabe, 2006, 2008b; Nakayama et al., 2006, 2010). For a multi-scaled model in the Tokyo area, hourly observation data from AMeDAS (Automated Meteorological Data Acquisition System) data (Japan Meteorological Agency, 2005-2006) were assimilated with the model. At the lateral boundaries of regional area, some meteorological data are input to the model from the ECMWF (European Centre for Medium-Range Weather Forecasts) with a resolution of 1°x 1° and from the MSM (Meso Scale Model) with a resolution of 10km x 10km (Japan Meteorological Agency, 2005-2006). Mean elevation was calculated by using a global digital elevation model (DEM; GTOPO30) (U.S. Geological Survey, 1996). Digital land cover data were categorized such as forests, grasses, bushes, shrubs, paddy fields, and cultivated fields. About 50 vegetation and soil parameters were calculated on the basis of vegetation class and soil maps (Chinese Academy of Sciences, 1988; Digital National Land Information GIS data of Japan, 2002). The geological structures were divided into four types on the basis of hydraulic conductivity, the specific storage of porous material, and specific yield by scanning and digitizing the geological material (Geological Atlas of China, 2002; Nakayama et al., 2007) and core-sampling data. Artificial augmentation of waterworks and sewerage systems, and anthropogenic sensible, latent, and sewage heats generated by buildings and factories were input into the model (Nakayama and Fujita, 2010; Nakayama and Hashimoto, 2011; Nakayama et al., 2007, 2012).

At the upstream boundaries, a reflecting condition on the hydraulic head was used assuming that there is no inflow from the mountains in the opposite direction (Nakayama and Watanabe, 2004). Time-series of tidal level was input as a variable head at the sea boundary (Nakayama, 2011a; Nakayama et al., 2006, 2007, 2010). Vertical geological structures were divided into 10–20 layers by using sample database. The hydraulic head values parallel to the ground level were input as the initial conditions. In river grids decided by digital river network, inflows or outflows from the riverbeds were simulated at each time step depending on the difference in the hydraulic heads of groundwater and river. The hydraulic head values parallel to the observed ground level were input as initial conditions for the groundwater sub-model. In river grids decided by digital river network from topographic maps, inflows or outflows from the riverbeds were simulated at each time step depending on the difference in the hydraulic heads of groundwater and river.

The simulation area covered 3,000 km by 2,000 km with a grid spacing of 10 km, covering the entire Changjiang and Yellow River Basins (Fig. 1). The vertical layer was discretized in thickness with depth, with each layer increased in thickness by a factor of 1.1 (Nakayama, 2011b; Nakayama and Watanabe, 2008b; Nakayama et al., 2006). In the Tokyo area, the simulation was conducted with multi-scaled levels in horizontally regional area (260 km wide by 260 km long with a grid spacing of 2 km covering Kanto region) nesting with one way to urban area (36 km wide by 26 km long with 200 m grid covering the Kawasaki City) (Nakayama and Hashimoto, 2011; Nakayama et al., 2007, 2012) (Fig. 1). These areas were discretized with a grid spacing of 200 m – 5 km in the horizontal direction. The NICE simulation was conducted on a NEC SX-8 supercomputer. The first 6 months were used as a warm-up period until equilibrium water levels were reached, and parameters were estimated by a comparison of simulated steady-state value with that published in previous literatures. A time step of the

simulation was changed from $\Delta t = 1.5$ sec to 1 h depending on spatial scale and the sub-model. Simulations were validated against various hydrothermal observed variables such as river discharge, soil moisture, groundwater level, air temperature, surface temperature, and heat-flux budget, et al.

3. Result and discussion

3.1. Effect of irrigation on hydrologic change

After the verification procedure (Nakayama, 2011b; Nakayama and Watanabe, 2008b), the model simulated effect of irrigation on evapotranspiration at rotation between winter wheat and summer maize in the downstream of Yellow River, and double-cropping of rice in the middle of Changjiang River (Fig. 3). Because more water is withdrawn during winter-wheat period due to small rainfall in the semi-arid north, the irrigation in this period affects greatly the increase in evapotranspiration (Fig. 3a), which is supplied by the limited water resources of river discharge and groundwater there. In particular, most of the irrigation is withdrawn from aquifer in the North China Plain (NCP) because surface water is seriously limited there (Nakayama, 2011a, 2011b; Nakayama et al., 2006). In the south, the irrigation is usually from the river to fill the paddy fiddle as ponding water depth (Nakayama, 2012c; Nakayama and Watanabe, 2008b), which increases evapotranspiration more in the drier season (Fig. 3b). This implies that energy supply is abundant relative to the water supply and the hydrological process is more sensitive to precipitation in the north, whereas the water supply is abundant relative to the energy supply and sun duration has a more significant impact in the south (Cong et al., 2010).

The model also simulated groundwater level in both Changjiang and Yellow River basins (Fig. 3c). The level decreases rapidly around the source area and the Qinghai Tibet Plateau, indicating that there are many sources of spring water in this region. The value is very low in the downstream because of the low elevation and overexploitation, in particular, in the NCP (Nakayama, 2011a, 2011b; Nakayama et al., 2006). This result indicates that hydrologic cycle including groundwater level is highly related not only to the topography but also to the irrigation water use. The NICE is effective to provide better evaluation of hydrological trends in longer period including 'evaporation paradox' (Roderick and Farquhar, 2002; Cong et al., 2010) together with observation networks because the model does not need the crop coefficient (depending on a growing stage and a kind of crop) for the calculation of actual evaporation and simulates it directly without detailed site-specific information or empirical relation to calculate effective precipitation (Nakayama, 2011a; Nakayama et al., 2006).

The mean TINDVI (Time-Integrated Normalized Difference Vegetation Index) gradients during 1982-1999 in various field crops (wheat, maize, and rice) at 4 stations were compared with trends of crop yields in the previous research (Tao et al., 2006) (Fig. 4a). The correlation of both values is relatively good ($r^2 = 0.986$) and the TINDVI gradient has a linear relation to the yield trend. The spatial pattern of the mean TINDVI gradient in agricultural fields shows a generally increasing tendency, particularly in the Yellow downstream and the NCP (Fig.

http://dx.doi.org/10.5772/52808

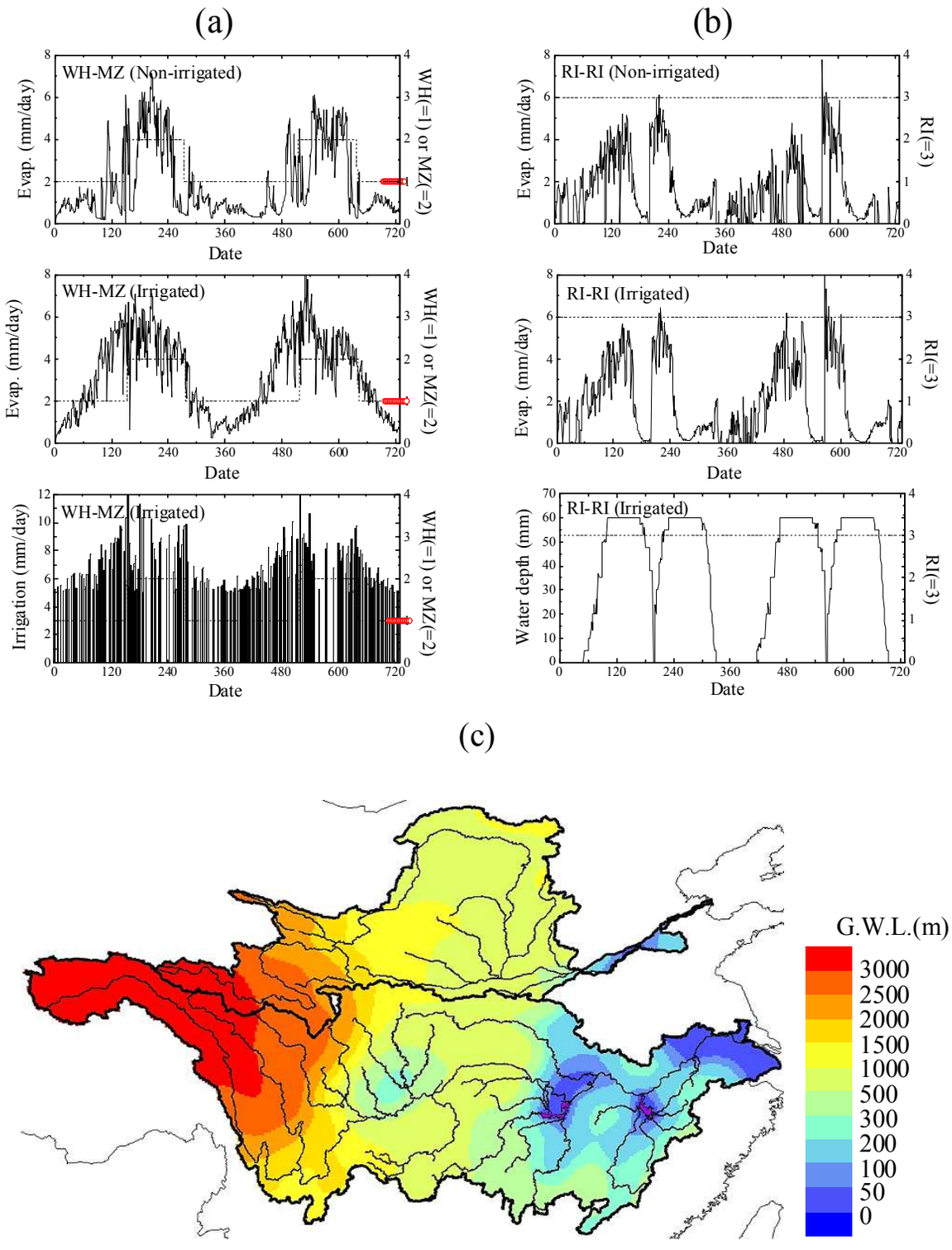

Figure 3. Impact of irrigation and ponding water depth on hydrological cycle; (a) evapotranspiration change at rotation between winter wheat and summer maize in the downstream of Yellow River, (b) evapotranspiration change at double-cropping of rice in the middle of Changjiang River, and (c) simulated results of annual-averaged groundwater level (a.s.l.) in the Changjiang and Yellow River basins. In Fig. 3a and 3b, right axis shows a period of each crop (WH; wheat, MZ; maize, and RI; rice, respectively).

4b), which is closely related to increasing tendency for winter wheat production in the downstream (U.S. Department of Agriculture, 1994), increase in irrigation water use (Yang et al., 2004) and chemical fertilizer, changes in crop varieties, improvements in technology such as agricultural machines, and other agronomic changes. On the other hand, it shows a generally decreasing tendency, particularly in the mid-lower reaches and around the lakes in the Changjiang River. This is caused mainly by an increase in lake reclamation, levee construction, and the resultant relative decrease in rice productivity in the lower reaches (Shankman and Liang, 2003; Zhao et al., 2005; Nakayama and Watanabe, 2008b). The decrease in the TINDVI gradient near the Bohai Sea, the East China Sea, and the Taihang Mountains was due to several effects including groundwater degradation, seawater intrusion, and rapid urbanization in the areas surrounding bigger cities (Brown and Halweil, 1998). Generally, these results suggest that the increase in irrigation water use is one of the reasons for the increase in crop production (Yang et al., 2004).

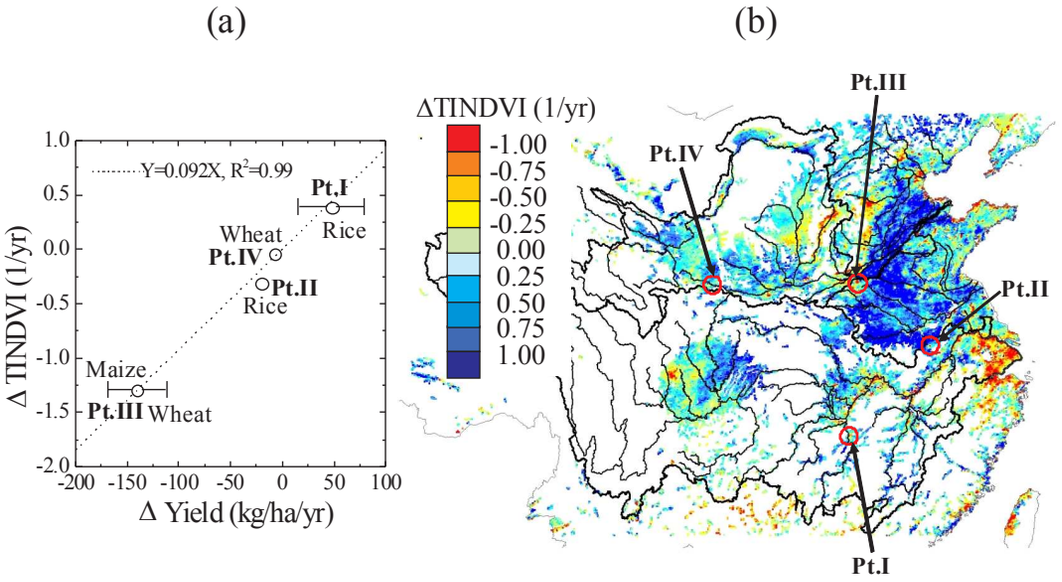

Figure 4. TINDVI over the agricultural fields by NOAA/AVHRR satellite images in the agricultural fields; (a) comparison of TINDVI with trend in observed yields at 4 stations (Pt.I; Changsha, Pt.II; Hefei, Pt.III; Zhengzhou, Pt.IV; Tianshui), and (b) spatial patterns in mean TINDVI gradient (per year) during 1982-1999.

3.2. Effective management of water resources to reduce urban heat island

The simulated heat-flux budget was compared at the infiltration and water-holding pavements after the verification with the analyzed value (Fig. 5). The water-holding pavement takes about 10.0 °C lower of the surface temperature than the infiltration pavement. The observed daily cycles of the road surface and air temperature at 1.5 m height were compared with those simulated by NICE after water irrigation in the same way as the previous research (Nakayama and Fujita, 2010). The model generally captured the observed water amount, and the associated diurnal cycle of the road surface and air temperature, and could estimate the temperature decrease trend with high accuracy. This cooling temperature is closely related to the promotion

http://dx.doi.org/10.5772/52808

of vaporization by using the water-holding pavement, and this trend continues during 5 days after the fulfillment of water-holding pavement. The rapid increase of latent heat (438 W/m^2) relative to sensible heat (127 W/m^2) was reported in the field observation at sprinkling roads (Yamagata et al., 2008). The simulated maximum sensible and latent heat fluxes in the water-holding pavement just after water irrigation were 130 W/m^2 and 345 W/m^2, which had relatively good approximations of 161 W/m^2 and 337 W/m^2 in observed values and this previous research. The model could simulate reasonably the general trend that the latent heat in the infiltration pavement was smaller than that in the water-holding pavement because the infiltration was more predominant than the evaporation.

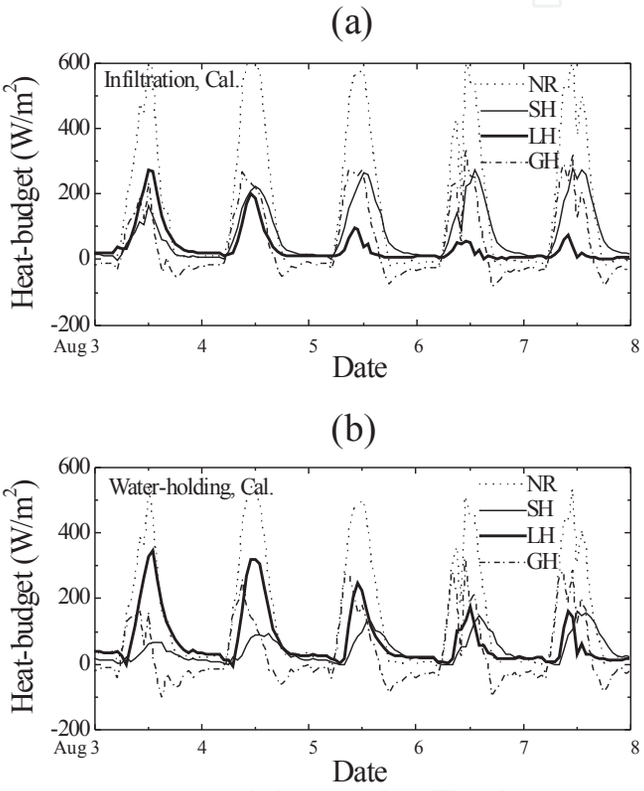

Figure 5. Simulated heat-flux budget in the symbiotic urban pavements after water irrigation at 3 August 2007; (a) infiltration pavement, and (b) water-holding pavement. Dotted line, net radiation (NR); solid line, sensible heat flux (SH); bold line, latent heat flux (LH); dash-dotted line, ground transfer heat flux (GH), respectively.

The author predicted the hydrothermal changes in the symbiotic urban scenarios (Fig. 6) (Nakayama and Hashimoto, 2011; Nakayama et al., 2012). NICE correctly predicted the much lower surface temperature of the water-holding block than those of the other pavements for several days after rainfall in comparison with simplified AUSSSM (Nakayama and Fujita, 2010), which was caused mainly by the rapid increase of evaporation after the rainfall (Fig. 6b). The predicted surface temperature on the scenario of water-holding pavement shows drastic decrease in the entire Kawasaki City (Fig. 6c). In particular, the business district beside the sea, where the urban heat island is predominant mainly due to the paved surface and the greater anthropogenic heat sources, has an effective cooling on this scenario.

The predicted groundwater level change in August is interesting in contrast to the simulated temperature (Fig. 6d). In the simulation on the scenario of water-holding pavement, all the necessary water to fill the water-holding pavement was automatically simulated by considering the difference between precipitation and evaporation, and withdrawn from the underneath groundwater in the NICE, which means that the pavement was always saturated. The groundwater level would decrease drastically at the commercial and industrial areas beside the sea and at the inland residential area, in exchange for a drastic cooling in the corresponding and the surrounding areas. The increase in recharge rate and the consequent increase in groundwater level on the scenario of a natural zone and green area are also effective to promote the groundwater resources in the urban area covered by impermeable pavement (Nakayama et al., 2007, 2012). The predicted temperature and groundwater level are greatly affected not only at the business district in the Kawasaki area but also at the Tokyo metropolitan area in the northern side of this study area. This result is very important from the political point of view, which indicates that we have to estimate more precisely the arrangement of symbiotic urban scenario in the study area together with the neighbouring administrations.

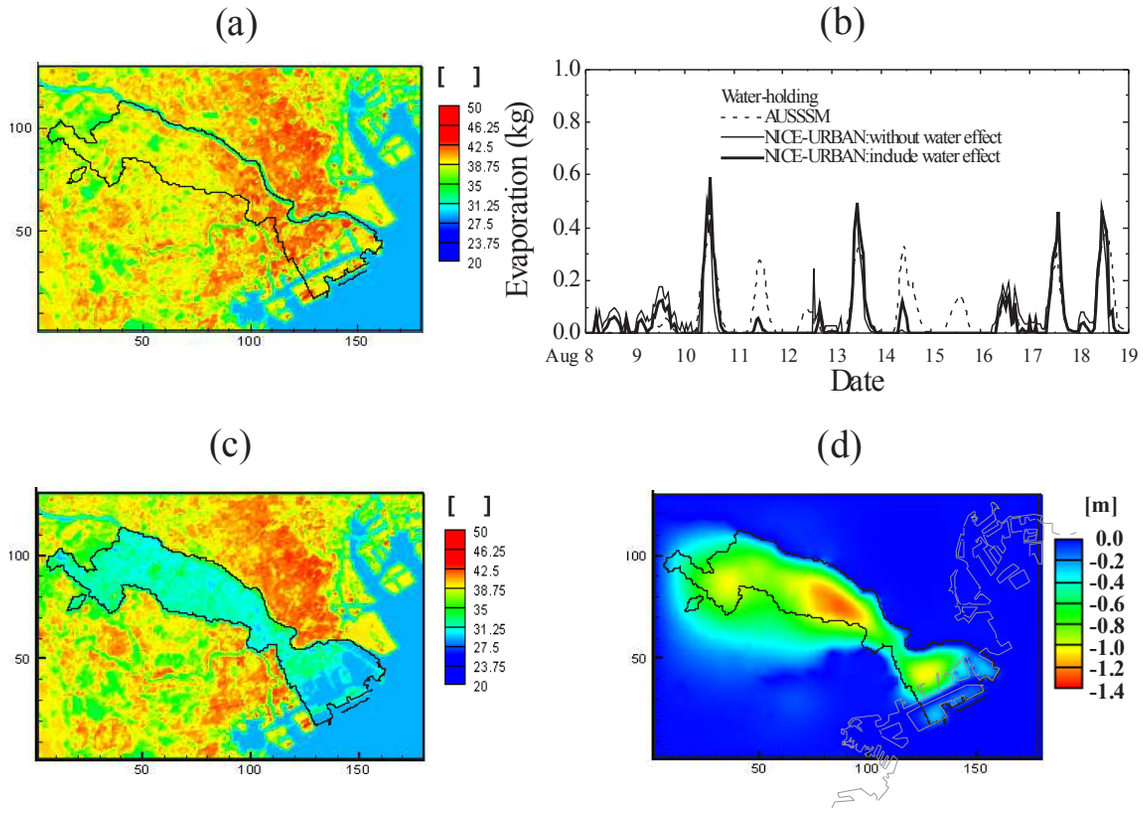

Figure 6. Prediction of hydrothermal changes at 5 August 2006; (a) present surface temperature, (b) evaporation simulated by NICE and simplified AUSSSM above water-holding pavement during 8-19 August 2006, and (c-d) predictions of surface temperature and groundwater level changes after water-holding pavement.

http://dx.doi.org/10.5772/52808

3.3. Discussion

Simulated results about the impact of irrigation on evapotranspiration change showed a clear difference between the Changjiang and Yellow Rivers. Because surface water and groundwater are administered separately by different authorities in China (Nakayama, 2011a), water management becomes further complicated if we consider it in both the Changjiang and Yellow Rivers. Any change in water accounting procedures may need to be negotiated through agreements brokered at relatively high levels of government, because surface water and groundwater are physically closely related to each other. The future development of irrigated and unirrigated fields and the associated crop production would affect greatly hydro-climate change and usable irrigation water from river and aquifer, and vice versa (Nakayama, 2011b). This research presented the lateral subsurface flow also has an important effect on the hydrologic cycle even in the continental scale, which extends traditional 'dynamic equilibrium' with atmospheric forcing (Maxwell and Kollet, 2008). From this point of view, nonstationarity models of relevant environmental variables have to be further developed to incorporate water infrastructure and water users including agricultural and energy sectors with a careful estimation of uncertainty (Milly et al., 2008).

This study also showed that the water-holding pavement scenario is effective for the urban area of floating subways, stations, and buildings in order to use moderately groundwater and to ameliorate the severe heat island through promotion of evaporation, whereas alternative land cover scenario of green area is also effective for the urban area of groundwater depression and seawater intrusion in order to promote the infiltration and to cool temperature. Therefore, the effective management of water resources including groundwater as a heat sink, particularly during the summer, would be attractive for both recovering a sound hydrologic cycle and tackling the urban heat island phenomenon (Ministry of Environment, 2004; Nakayama et al., 2007, 2012), so-called, 'Win-Win' approach. We are convinced that integrated management of both surface water and groundwater by using NICE in a political scenario for the effective selection and use of ecosystem service sites (Millennium Ecosystem Assessment, 2005) would play an important role in the creation of thermally-pleasing environments and the achievement in sustainable development in urban regions.

Recently, environmental pollution is becoming intertwined with various aspects (Fig. 7). Land subsidence is still a serious environmental problem around the foot of mountain near the Tokyo Metropolis due to delayed regulatory enforcement and continuation of extensive groundwater extraction. Water contaminant also shows some relation to this heterogeneity in addition to the thermal environment through complex chemical reaction, which implies further importance to evaluate these problems synthetically. Present result indicates effective management of water resource including evapotranspiration is also powerful for mitigation of heat island, which implies a possibility of achieving win-win solution about hydrothermal pollutions in eco-conscious society. The procedure to construct integrated assessment system would be also valuable for adaptation to climate change and urbanization in global scale, proposal of sustainability index, and providing eco-conscious society (Ministry of Environment, 2004; Nakayama and Hashimoto, 2011; Nakayama et al., 2007, 2012).

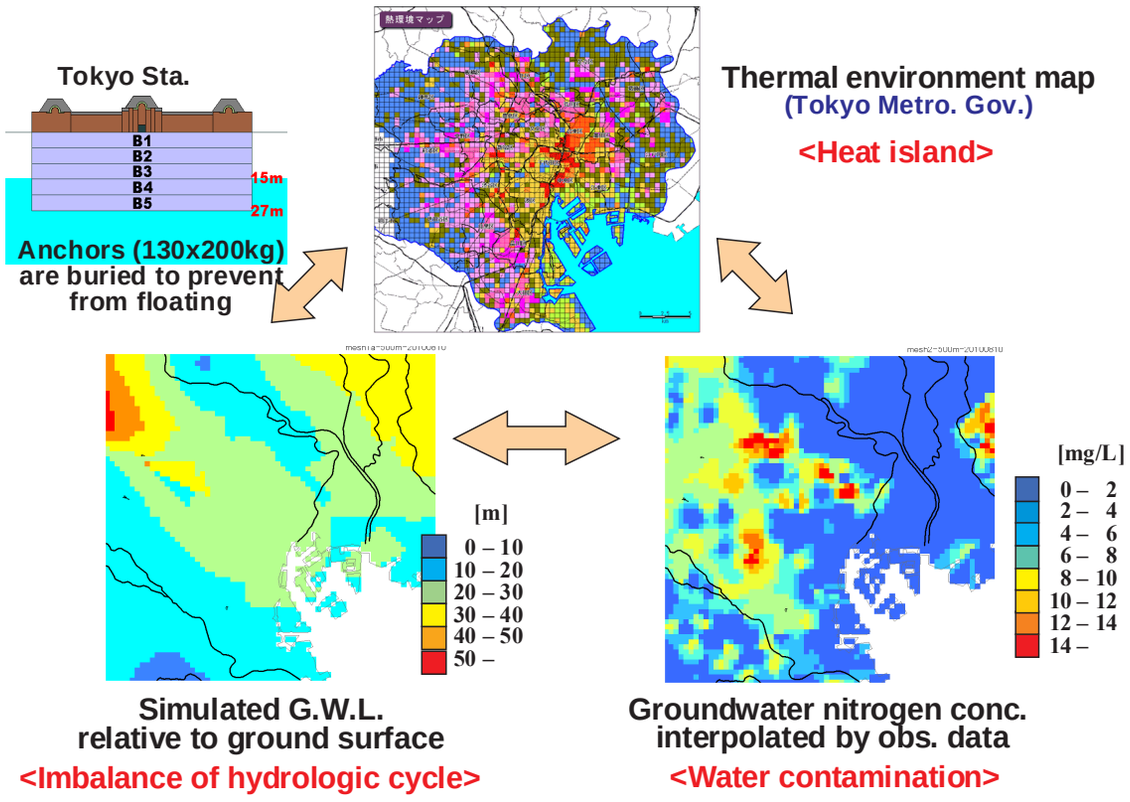

Figure 7. Intertwined environmental pollution in urban and surrounding areas.

4. Conclusion

This study coupled National Integrated Catchment-based Eco-hydrology (NICE) model series with complex sub-models to develop coupled human and natural systems and to analyze impact of evapotranspiration on hydrothermal changes in regional scale. The model includes different functions of representative crops (wheat, maize, soybean, and rice) and simulates automatically dynamic growth processes and biomass formulation. The simulated result showed impact of irrigation on eco-hydrological processes. The spatial pattern of Time-Integrated NDVI (TINDVI) gradient in agricultural fields indicated heterogeneous characteristics of crop yield, which implied the increase in irrigation water use is one of the reasons for the increase in crop production. NICE also reproduced reasonably the observed hydrothermal characteristics including the water and heat budgets in various pavements, evaluated the role of a new surface material (water-holding pavement) in promoting evaporation and cooling temperature to counter the urban heat island phenomenon, and predicted the hydrothermal changes under alternative land cover scenarios. These results suggest strongly the needs of trans-boundary and multi-disciplinary solutions of water management for sustainable development under sound socio-economic conditions contributory to national and global securities.

Acknowledgements

The author thanks Dr. M. Watanabe, Keio University, Japan, Dr. Y. Yang, Shijiazhuang Institute of Agricultural Modernization of the Chinese Academy of Sciences (CAS), China, and Dr. K. Xu, National Institute for Environmental Studies (NIES), Japan, for valuable comments about the study areas. Some of the simulations in this study were run on an NEC SX–8 supercomputer at the Center for Global Environmental Research (CGER), NIES. The support of the Environmental Technology Development Fund from the Japanese Ministry of Environment is also acknowledged.

Author details

Tadanobu Nakayama[1,2]

1 National Institute for Environmental Studies (NIES), Onogawa, Tsukuba, Ibaraki, Japan

2 Centre for Ecology & Hydrology (CEH), Crowmarsh Gifford, Wallingford, Oxfordshire, UK

References

[1] Brown, L. R, & Halweil, B. (1998). China's water shortage could shake world food security. *World Watch*, 0896-0615, 11, 10-18.

[2] Chang, C. R, Li, M. H, & Chang, S. D. (2007). A preliminary study on the local cool-island intensity of Taipei city parks. *Landscape Urban Plan.*, 0169-2046, 80, 386-395.

[3] Chinese Academy of Sciences(1988). *Administrative division coding system of the People's Republic of China*, Beijing

[4] Cong, Z, Zhao, J, Yang, D, & Ni, G. (2010). Understanding the hydrological trends of river basins in China. *J. Hydrol.*, doi:j.jhydrol.2010.05.013, 0022-1694, 388, 350-356.

[5] Digital National Land Information GIS Data of Japan(2002). *Database of groundwater in Japan.* Ministry of Land Infrastructure and Transport of Japan, http://www.nla.go.jp/ksj/

[6] Geological Atlas of China(2002). Geological Publisher, Beijing (in Chinese)

[7] Japan Meteorological Agency (JMA)(2005). *AMeDAS (Automated Meteorological Data Acquisition System) Annual Reports 20052006*Japan Meteorological Business Support Center (CD-ROM)

[8] Japan Meteorological Agency (JMA)(2005). *MSM (Meso Scale Model) Objective Analysis Data 20052006*Japan Meteorological Business Support Center (CD-ROM)

[9] Maxwell, R. M, & Kollet, S. J. (2008). Interdependence of groundwater dynamics and land-energy feedbacks under climate change. *Nat. Geosci.*, doi:ngeo315, 1752-0894, 1, 665-669.

[10] Millennium Ecosystem Assessment(2005). *Strengthening capacity to manage ecosystems sustainability for human well-being*, http://www.millenniumassessment.org/en/index.aspx

[11] Milly, P. C. D, Betancourt, J, Falkenmark, M, Hirsch, R. M, Kundzewicz, Z. W, Lettenmaier, D. P, & Stouffer, R. J. (2008). Stationarity is dead: Whither water management ?. *Science*, doi:science.1151915, 0036-8075, 319, 573-574.

[12] Ministry of Environment(2004). *Report on heat-island measures by controlling anthropogenic exhaustion heat in the urban area*, http://www.env.go.jp/air/report/hin Japanese)

[13] Nakayama, T, & Watanabe, M. (2004). Simulation of drying phenomena associated with vegetation change caused by invasion of alder (Alnus japonica) in Kushiro Mire. *Water Resour. Res.*, W08402, doi:WR003174, 0043-1397, 40

[14] Nakayama, T, & Watanabe, M. (2006). Simulation of spring snowmelt runoff by considering micro-topography and phase changes in soil layer. *Hydrol. Earth Syst. Sci. Discuss.*, 1027-5606, 3, 2101-2144.

[15] Nakayama, T, Yang, Y, Watanabe, M, & Zhang, X. (2006). Simulation of groundwater dynamics in North China Plain by coupled hydrology and agricultural models. *Hydrol. Process.*, doi:hyp.6142, 0885-6087, 20, 3441-3466.

[16] Nakayama, T, Watanabe, M, Tanji, K, & Morioka, T. (2007). Effect of underground urban structures on eutrophic coastal environment. *Sci. Total Environ.*, doi:j.scitotenv.2006.11.033, 0048-9697, 373, 270-288.

[17] Nakayama, T. (2008a). Factors controlling vegetation succession in Kushiro Mire. *Ecol. Model.*, doi:j.ecolmodel.2008.02.017, 0304-3800, 215, 225-236.

[18] Nakayama, T. (2008b). Shrinkage of shrub forest and recovery of mire ecosystem by river restoration in northern Japan. *Forest Ecol. Manag.*, doi:j.foreco.2008.07.017, 0378-1127, 256, 1927-1938.

[19] Nakayama, T, & Watanabe, M. (2008a). Missing role of groundwater in water and nutrient cycles in the shallow eutrophic Lake Kasumigaura, Japan. *Hydrol. Process.*, doi:hyp.6684, 0885-6087, 22, 1150-1172.

[20] Nakayama, T, & Watanabe, M. (2008b). Role of flood storage ability of lakes in the Changjiang River catchment. *Global Planet. Change*, doi:j.gloplacha.2008.04.002, 0921-8181, 63, 9-22.

[21] Nakayama, T, & Watanabe, M. (2008c). Modelling the hydrologic cycle in a shallow eutrophic lake. *Verh. Internat. Verein. Limnol.*, 0368-0770, 30, 345-348.

[22] Nakayama, T. (2009). Simulation of Ecosystem Degradation and its Application for Effective Policy-Making in Regional Scale, In: *River Pollution Research Progress*, Mattia

N. Gallo & Marco H. Ferrari (Eds.), Nova Science Publishers, Inc., 978-1-60456-643-7New York, 1-89.

[23] Nakayama, T. (2010). Simulation of hydrologic and geomorphic changes affecting a shrinking mire. *River Res. Appl.*, doi:rra.1253, 1535-1459, 26, 305-321.

[24] Nakayama, T, & Fujita, T. (2010). Cooling effect of water-holding pavements made of new materials on water and heat budgets in urban areas. *Landscape Urban Plan.*, doi:j.landurbplan.2010.02.003, 0169-2046, 96, 57-67.

[25] Nakayama, T, Sun, Y, & Geng, Y. (2010). Simulation of water resource and its relation to urban activity in Dalian City, Northern China. *Global Planet. Change*, doi:j.gloplacha. 2010.06.001, 0921-8181, 73, 172-185.

[26] Nakayama, T. (2011a). Simulation of complicated and diverse water system accompanied by human intervention in the North China Plain. *Hydrol. Process.*, doi:hyp.8009, 0885-6087, 0885-6087.

[27] Nakayama, T. (2011b). Simulation of the effect of irrigation on the hydrologic cycle in the highly cultivated Yellow River Basin. *Agr. Forest Meteorol.*, doi:j.agrformet. 2010.11.006, 0168-1923, 151, 314-327.

[28] Nakayama, T, & Hashimoto, S. (2011). Analysis of the ability of water resources to reduce the urban heat island in the Tokyo megalopolis. *Environ. Pollut.*, doi:j.envpol. 2010.11.016, 0269-7491, 159, 2164-2173.

[29] Nakayama, T. (2012a). Visualization of missing role of hydrothermal interactions in Japanese megalopolis for win-win solution. *Water Sci. Technol.*, doi:wst.2012.205, 0273-1223, 66, 409-414.

[30] Nakayama, T. and regime shift of mire ecosystem in northern Japan. *Hydrol. Process.*, doi:hyp.9347, 0885-6087, 26, 2455-2469.

[31] Nakayama, T. (2012c). Impact of anthropogenic activity on eco-hydrological process in continental scales. *Proc. Environ. Sci.*, doi:j.proenv.2012.01.008, 1878-0296, 13, 87-94.

[32] Nakayama, T, Hashimoto, S, & Hamano, H. (2012). Multi-scaled analysis of hydrothermal dynamics in Japanese megalopolis by using integrated approach. *Hydrol. Process.*, doi:hyp.9290, 0885-6087, 26, 2431-2444.

[33] Oke, T. R. (1987). *Boundary layer climates*, Methuen Press, 978-0-41504-319-9London.

[34] Pielke, R. A, Cotton, W. R, Walko, R. L, Tremback, C. J, Lyons, W. A, Grasso, L. D, Nicholls, M. E, Moran, M. D, Wesley, D. A, Lee, T. J, & Copeland, J. H. (1992). A omprehensive meteorological modeling system-RAMS. *Meteorol. Atmos. Phys.*, 0177-7971, 49, 69-91.

[35] Priestley, C. H. B, & Taylor, R. J. (1972). On the assessment of surface heat flux and evaporation using large-scale parameters. *Mon. Weather Rev.*, 0027-0644, 100, 81-92.

[36] Ritchie, J. T, Singh, U, Godwin, D. C, & Bowen, W. T. (1998). Cereal growth, development and yield, In: *Understanding Options for Agricultural Production*, Tsuji, G.Y., Hoogenboom, G. & Thornton, P.K. (Eds.), Kluwer, 0-79234-833-8Britain, 79-98.

[37] Roderick, M. L, & Farquhar, G. D. (2002). The cause of decreased pan evaporation over the past 50 years. *Science*, 0036-8075, 298, 1410-1411.

[38] Sellers, P. J, Randall, D. A, Collatz, G. J, Berry, J. A, Field, C. B, Dazlich, D. A, Zhang, C, Collelo, G. D, & Bounoua, L. (1996). A revised land surface prameterization (SiB2) for atomospheric GCMs. Part I : Model formulation. *J. Climate*, 0894-8755, 9, 676-705.

[39] Shankman, D, & Liang, Q. (2003). Landscape changes and increasing flood frequency in China's Poyang Lake region. *Prof. Geogr.*, 0033-0124, 55, 434-445.

[40] Spronken-smith, R. A, & Oke, T. R. (1999). Scale modeling of nocturnal cooling in urban parks. Boundary-Layer Meteorology 0006-8314, 93, 287-312.

[41] Tao, F, Yokozawa, M, Xu, Y, Hayashi, Y, & Zhang, Z. (2006). Climate changes and trends in phenology and yields of field crops in China, 1981-2000. *Agr. Forest Meteorol.*, 0168-1923, 138, 82-92.

[42] U.S. Department of Agriculture (USDA). (1994). *Major World Crop Areas and Climatic Profiles*. World Agricultural Outlook Board, USDA, Agricultural Handbook No.664, http://www.usda.gov/oce/weather/pubs/Other/MWCACP/MajorWorldCropAreas.pdf

[43] U.S. Geological Survey. (1996). *GTOPO30 Global 30 Arc Second Elevation Data Set*, USGS, http://www1.gsi.go.jp/geowww/globalmap-gsi/gtopo30/gtopo30.html

[44] Yamagata, H, Nasu, M, Yoshizawa, M, Miyamoto, A, & Minamiyama, M. (2008). Heat island mitigation using water retentive pavement sprinkled with reclaimed wastewater. *Water Sci. Technol.*, doi:wst.2008.187, 0273-1223, 57, 763-771.

[45] Yang, D, Li, C, Hu, H, Lei, Z, Yang, S, Kusuda, T, Koike, T, & Musiake, K. (2004). Analysis of water resources variability in the Yellow River of China during the last half century using historical data. *Water Resour. Res.*, W06502, doi:WR002763, 0043-1397, 40

[46] Zhao, S, Fang, J, Miao, S, Gu, B, Tao, S, Peng, C, & Tang, Z. (2005). The 7-decade degradation of a large freshwater lake in central Yangtze River, China. *Environ. Sci. Technol.*, 0001-3936X, 39, 431-436.